




# Form factors and two-photon exchange in high-energy elastic electron-proton scattering

M. E. Christy,<sup>1</sup> T. Gautam,<sup>1</sup> L. Ou,<sup>2</sup> B. Schmookler,<sup>2</sup> Y. Wang,<sup>3</sup> D. Adikaram,<sup>4</sup> Z. Ahmed,<sup>5</sup> H. Albataineh,<sup>6</sup> S. F. Ali,<sup>7</sup> B. Aljawrneh,<sup>8</sup> K. Allada,<sup>2</sup> S.L. Allison,<sup>9</sup> S. Alsalmi,<sup>10</sup> D. Androic,<sup>11</sup> K. Aniol,<sup>12</sup> J. Annand,<sup>13</sup> J. Arrington,<sup>14,15</sup> H. Atac,<sup>16</sup> T. Averett,<sup>3</sup> C. Ayerbe Gayoso,<sup>3</sup> X. Bai,<sup>17</sup> J. Bane,<sup>18</sup> S. Barcus,<sup>3</sup> K. Bartlett,<sup>3</sup> V. Bellini,<sup>19</sup> R. Beminiwattha,<sup>20</sup> J. Bericic,<sup>4</sup> H. Bhatt,<sup>21</sup> D. Bhetuwal,<sup>21</sup> D. Biswas,<sup>1</sup> E. Brash,<sup>22</sup> D. Bulumulla,<sup>9</sup> C. M. Camacho,<sup>23</sup> J. Campbell,<sup>24</sup> A. Camsonne,<sup>4</sup> M. Carmignotto,<sup>7</sup> J. Castellanos,<sup>25</sup> C. Chen,<sup>1</sup> J-P. Chen,<sup>4</sup> T. Chetry,<sup>26</sup> E. Cisbani,<sup>27</sup> B. Clary,<sup>28</sup> E. Cohen,<sup>29</sup> N. Compton,<sup>26</sup> J. C. Cornejo,<sup>3,30</sup> S. Covrig Dusa,<sup>4</sup> B. Crowe,<sup>31</sup> S. Danagoulian,<sup>8</sup> T. Danley,<sup>26</sup> W. Deconinck,<sup>3</sup> M. Defurne,<sup>32</sup> C. Desnault,<sup>23</sup> D. Di,<sup>17</sup> M. Dlamini,<sup>26</sup> M. Duer,<sup>29</sup> B. Duran,<sup>16</sup> R. Ent,<sup>4</sup> C. Fanelli,<sup>2</sup> E. Fuchey,<sup>28</sup> C. Gal,<sup>17</sup> D. Gaskell,<sup>4</sup> F. Georges,<sup>33</sup> S. Gilad,<sup>2</sup> O. Glamazdin,<sup>34</sup> K. Gnanvo,<sup>17</sup> A. V. Gramolin,<sup>35</sup> V. M. Gray,<sup>3</sup> C. Gu,<sup>17</sup> A. Habarakada,<sup>1</sup> T. Hague,<sup>10</sup> G. Hamad,<sup>26</sup> D. Hamilton,<sup>13</sup> K. Hamilton,<sup>13</sup> O. Hansen,<sup>4</sup> F. Hauenstein,<sup>9</sup> A. V. Hernandez,<sup>7</sup> W. Henry,<sup>16</sup> D. W. Higinbotham,<sup>4</sup> T. Holmstrom,<sup>36</sup> T. Horn,<sup>7</sup> Y. Huang,<sup>17</sup> G.M. Huber ,<sup>5</sup> C. Hyde,<sup>9</sup> H. Ibrahim,<sup>37</sup> N. Israel,<sup>26</sup> C-M. Jen,<sup>38</sup> K. Jin,<sup>17</sup> M. Jones,<sup>4</sup> A. Kabir,<sup>10</sup> B. Karki,<sup>26</sup> C. Keppel,<sup>4</sup> V. Khachatryan,<sup>39,40</sup> P.M. King,<sup>26</sup> S. Li,<sup>41</sup> W. Li,<sup>5</sup> H. Liu,<sup>42</sup> J. Liu,<sup>17</sup> A. H. Liyanage,<sup>1</sup> D. Mack,<sup>4</sup> J. Magee,<sup>3</sup> S. Malace,<sup>4</sup> J. Mammei,<sup>43</sup> P. Markowitz,<sup>25</sup> S. Mayilyan,<sup>44</sup> E. McClellan,<sup>4</sup> F. Meddi,<sup>27</sup> D. Meekins,<sup>4</sup> K. Mesick,<sup>45</sup> R. Michaels,<sup>4</sup> A. Mkrtchyan,<sup>7</sup> B. Moffit,<sup>4</sup> R. Montgomery,<sup>13</sup> L.S. Myers,<sup>4</sup> P. Nadel-Turonski,<sup>4</sup> S. J. Nazeer,<sup>1</sup> V. Nelyubin,<sup>17</sup> D. Nguyen,<sup>17</sup> N. Nuruzzaman,<sup>1</sup> M. Nycz,<sup>10</sup> R.F. Obrecht,<sup>28</sup> K. Ohanyan,<sup>44</sup> C. Palatchi,<sup>17</sup> B. Pandey,<sup>1</sup> K. Park,<sup>9</sup> S. Park,<sup>39</sup> C. Peng,<sup>46</sup> F. D. Persio,<sup>27</sup> R. Pomatsalyuk,<sup>34</sup> E. Pooser,<sup>4</sup> A.J.R. Puckett,<sup>28</sup> V. Punjabi,<sup>47</sup> B. Quinn,<sup>30</sup> S. Rahman,<sup>43</sup> M.N.H. Rashad,<sup>9</sup> P.E. Reimer ,<sup>15</sup> S. Riordan,<sup>39</sup> J. Roche,<sup>26</sup> I. Sapkota,<sup>7</sup> A. Sarty,<sup>48</sup> B. Sawatzky,<sup>4</sup> N. H. Saylor,<sup>49</sup> M. H. Shabestari,<sup>21</sup> A. Shahinyan,<sup>44</sup> S. Širca,<sup>50</sup> G.R. Smith,<sup>4</sup> S. Sooriyaarachchilage,<sup>1</sup> N. Sparveris,<sup>16</sup> R. Spies,<sup>43</sup> A. Stefanko,<sup>30</sup> T. Su,<sup>10</sup> A. Subedi,<sup>21</sup> V. Sulkosky,<sup>2</sup> A. Sun,<sup>30</sup> Y. Tan,<sup>51</sup> L. Thorne,<sup>30</sup> N. Ton,<sup>17</sup> F. Tortorici,<sup>19</sup> R. Trotta,<sup>52</sup> R. Uniyal,<sup>7</sup> G.M. Urciuoli,<sup>27</sup> E. Voutier,<sup>23</sup> B. Waidyawansa,<sup>4</sup> B. Wojtsekhowski ,<sup>4,\*</sup> S. Wood,<sup>4</sup> X. Yan,<sup>53</sup> L. Ye,<sup>21</sup> Z. H. Ye,<sup>17</sup> C. Yero,<sup>25</sup> J. Zhang,<sup>17</sup> Y. X. Zhao,<sup>39</sup> and P. Zhu<sup>54</sup>

<sup>1</sup>Hampton University, Hampton, Virginia 23669, USA

<sup>2</sup>Massachusetts Institute of Technology, Cambridge, Massachusetts 02139, USA

<sup>3</sup>William and Mary, Williamsburg, Virginia 23185, USA

<sup>4</sup>Thomas Jefferson National Accelerator Facility, Newport News, Virginia 23606, USA

<sup>5</sup>University of Regina, Regina, SK, S4S 0A2 Canada

<sup>6</sup>Texas A & M University, Kingsville, Texas 77843, USA

<sup>7</sup>Catholic University of America, Washington, DC 20064, USA

<sup>8</sup>North Carolina Ag. and Tech. St. Univ., Greensboro, North Carolina 27411, USA

<sup>9</sup>Old Dominion University, Norfolk, Virginia 23529, USA

<sup>10</sup>Kent State University, Kent, Ohio 44240, USA

<sup>11</sup>University of Zagreb, Trg Republike Hrvatske 14, 10000, Zagreb, Croatia

<sup>12</sup>California State University, Los Angeles, Los Angeles, California 90032, USA

<sup>13</sup>SUPA School of Physics and Astronomy, University of Glasgow, Glasgow G12 8QQ, UK

<sup>14</sup>Lawrence Berkeley National Laboratory, Berkeley, California 94720, USA

<sup>15</sup>Argonne National Laboratory, Lemont, Illinois 60439, USA

<sup>16</sup>Temple University, Philadelphia, Pennsylvania 19122, USA

<sup>17</sup>University of Virginia, Charlottesville, Virginia 22904, USA

<sup>18</sup>University of Tennessee, Knoxville, Tennessee 37996, USA

<sup>19</sup>Istituto Nazionale di Fisica Nucleare, Dipt. di Fisica dell Univ. di Catania, I-95123 Catania, Italy

<sup>20</sup>Syracuse University, Syracuse, New York, 13244, USA

<sup>21</sup>Mississippi State University, Mississippi State, Mississippi 39762, USA

<sup>22</sup>Christopher Newport University, Newport News, Virginia 23606, USA

<sup>23</sup>Institut de Physique Nucleaire, 15 Rue Georges Clemenceau, 91400 Orsay, France

<sup>24</sup>Dalhousie University, Nova Scotia, NS B3H 4R2, Canada

<sup>25</sup>Florida International University, Miami, Florida 33199, USA

<sup>26</sup>Ohio University, Athens, Ohio 45701, USA

<sup>27</sup>Istituto Nazionale di Fisica Nucleare - Sezione di Roma, P.le Aldo Moro, 2 - 00185 Roma, Italy

<sup>28</sup>University of Connecticut, Storrs, Connecticut 06269, USA

<sup>29</sup>Tel Aviv University, Tel Aviv-Yafo, Israel

<sup>30</sup>Carnegie Mellon University, Pittsburgh, Pennsylvania 15213, USA

<sup>31</sup>North Carolina Central University, Durham, North Carolina 27707, USA

<sup>32</sup>CEA Saclay, 91191 Gif-sur-Yvette, France

<sup>33</sup>Ecole Centrale Paris, 3 Rue Joliot Curie, 91190 Gif-sur-Yvette, France

<sup>34</sup>Kharkov Institute of Physics and Technology, Kharkov 61108, Ukraine

<sup>35</sup>Boston University, Boston, Massachusetts 02215, USA

<sup>36</sup>Randolph Macon College, Ashland, Virginia 23005, USA

- <sup>37</sup>Cairo University, Cairo, 12613, Egypt  
<sup>38</sup>Virginia Polytechnic Inst. & State Univ., Blacksburg, Virginia 234061, USA  
<sup>39</sup>Stony Brook, State University of New York, New York 11794, USA  
<sup>40</sup>Cornell University, Ithaca, New York 14853, USA  
<sup>41</sup>University of New Hampshire, Durham, New Hampshire 03824, USA  
<sup>42</sup>Columbia University, New York, New York 10027, USA  
<sup>43</sup>University of Manitoba, Winnipeg, MB R3T 2N2, Canada  
<sup>44</sup>AANL, 2 Alikhanian Brothers Street, 0036, Yerevan, Armenia  
<sup>45</sup>Rutgers University, New Brunswick, New Jersey 08854, USA  
<sup>46</sup>Duke University, Durham, North Carolina 27708, USA  
<sup>47</sup>Norfolk State University, Norfolk, Virginia 23504, USA  
<sup>48</sup>Saint Mary's University, Halifax, Nova Scotia B3H 3C3, Canada  
<sup>49</sup>Rensselaer Polytechnic Institute, Troy, New York 12180, USA  
<sup>50</sup>Faculty of Mathematics and Physics, University of Ljubljana, 1000 Ljubljana, Slovenia  
<sup>51</sup>Shandong University, Jinan, China  
<sup>52</sup>Duquesne University, Pittsburgh, Pennsylvania 15282, USA  
<sup>53</sup>Huangshan University, Tunxi, Daizhen Rd, China  
<sup>54</sup>University of Science and Technology of China, Hefei, Anhui 230026, China  
(Dated: March 24, 2021)

We report new precision measurements of the elastic electron-proton scattering cross section for momentum transfer squared ( $Q^2$ ) up to  $15.75 \text{ (GeV/c)}^2$ . These data allow for improved extraction of the proton magnetic form factor at high  $Q^2$  and nearly double the  $Q^2$  range of direct longitudinal/transverse separated cross sections. A comparison of our results to polarization measurements establishes the presence of hard two-photon exchange in the  $e$ - $p$  elastic scattering cross section at greater than 95% confidence level for  $Q^2$  up to  $8 \text{ (GeV/c)}^2$ .

PACS numbers: 25.30.Bf, 13.40.Gp, 14.20.Dh

Elastic electron scattering is a key process used in studies of matter across a wide range of energy scales and in many sub-fields of physics. In the one-photon exchange approximation (OPE), first calculated in Ref. [1], the differential electron-nucleon elastic scattering cross section,  $d\sigma(\theta_e)/d\Omega_e$ , is the product of the cross section for a structureless object and a structure-dependent term that depends on the Sachs magnetic and electric form factors [2],  $G_M(Q^2)$  and  $G_E(Q^2)$ , which encode the spatial distributions of magnetization and charge in the proton:

$$\frac{d\sigma(\theta_e)}{d\Omega_e} = \frac{d\sigma_{\text{Mott}}}{d\Omega_e} \cdot \frac{\tau G_M^2(Q^2) + \varepsilon G_E^2(Q^2)}{\varepsilon(1 + \tau)}. \quad (1)$$

In Eq. (1),  $\theta_e$  is the scattering angle of the electron,  $d\sigma_{\text{Mott}}/d\Omega_e$  is the cross section for scattering of an electron with incident (scattered) energy  $E_e$  ( $E'_e$ ) from a structureless target,  $Q^2 = 4E_e E'_e \sin^2(\theta_e/2)$  is the negative four-momentum transfer squared,  $\varepsilon \equiv [1 + 2(1 + \tau) \tan^2(\theta_e/2)]^{-1}$  is the virtual photon polarization parameter, and  $\tau \equiv Q^2/4M_p^2$ . The structure-dependent term is isolated in the reduced cross section,

$$\begin{aligned} \sigma_R &= \tau G_M^2(Q^2) + \varepsilon G_E^2(Q^2) = \sigma_T + \varepsilon \sigma_L \\ &= G_M^2(Q^2)(\tau + \varepsilon \text{RS}(Q^2)/\mu_p^2), \end{aligned} \quad (2)$$

where  $\sigma_L$  and  $\sigma_T$  are the longitudinal and transverse contributions to the cross section, respectively,  $\text{RS} = (\mu_p G_E/G_M)^2$  is the normalized Rosenbluth slope, and  $\mu_p$  is the proton magnetic moment. The form factors can be extracted using measurements at fixed  $Q^2$  but different values of  $\varepsilon$ , corresponding

to different electron scattering angles. A linear fit to measurements of  $\sigma_R(\varepsilon)$  yields an intercept of  $\sigma_R(\varepsilon = 0) = \tau G_M^2$ , and a slope of  $d\sigma_R/d\varepsilon = G_E^2$ . This method is commonly known as Rosenbluth or Longitudinal/Transverse (L/T) separation.

Pioneering measurements of elastic electron-proton scattering by R. Hofstadter [3] confirmed the theoretical expectation of linear dependence of  $\sigma_R$  as a function of  $\varepsilon$ , which supported the use of the OPE approximation. Additional measurements, including one in Ref. [4], extended linearity tests up to  $Q^2 = 3 \text{ (GeV/c)}^2$  and demonstrated that  $G_E$  and  $G_M$  both approximately follow the dipole form  $G_D \equiv (1 + Q^2/\Lambda^2)^{-2}$ , with  $\Lambda^2 = 0.71 \text{ GeV}^2$ , yielding form factor scaling:  $\mu_p G_E/G_M \approx 1$ . At larger  $Q^2$  values,  $\tau$  enhances the contribution from  $G_M$ , making it difficult to extract  $G_E$  using the Rosenbluth method. Elastic cross section analyses at higher  $Q^2$  values [5, 6] extracted  $G_M$  under the assumption that  $\text{RS} = 1$ . These data showed that  $Q^4 G_M(Q^2)$  was  $Q^2$ -independent above  $10 \text{ (GeV/c)}^2$ , consistent with the pQCD prediction [7].

The reduced sensitivity to  $G_E^2$  at high  $Q^2$  in the Rosenbluth method motivated the use of double polarization observables [8], for which the OPE formalism was developed in Refs. [8–11]. Polarization measurements are directly sensitive to the ratio  $G_E/G_M$ , but not to the individual form factors. About 20 years ago the first precision measurements were performed [12] and a novel effect was discovered: the form factor ratio (FFR) extracted from polarization data decreased dramatically with  $Q^2$ , see Refs. [12–14].

The decrease of the FFR with increasing  $Q^2$  revealed unexpected new physics, with proposed explanations ranging from the role of quark orbital momentum [15] to the effect of the di-

quark correlation in the nucleon ground state [16]. In addition, the discrepancy between the FFR extracted from polarization measurements and from cross sections was surprising, and requires deeper understanding. This discrepancy is referred to henceforth as the form factor ratio puzzle (FFRP).

Soon after the FFRP was discovered, two experiments were proposed involving detection of the struck proton [17, 18], whose constant momentum at a given  $Q^2$  allows reduction of instrumentation systematics. A reanalysis of the world data [19], and new measurements of RS values with both scattered electron detection [20] and recoil proton detection [21], confirmed with improved precision the original experimental results from the Rosenbluth method of an approximately constant value of RS at  $Q^2$  up to  $5.5 \text{ (GeV/c)}^2$ .

The leading explanation of the FFRP is the contribution from hard two-photon exchange (TPE) to the  $e$ - $p$  elastic scattering cross section [22, 23]. TPE effects can change the slope of  $\sigma_R$  vs.  $\epsilon$  and introduce non-linear contributions in the reduced cross section. At large  $Q^2$  values, where the slope arising from  $G_E$  is extremely small, even a small change in the slope can lead to a large fractional change in the RS. A non-linearity of the reduced cross section as a function of  $\epsilon$  was explored for a TPE signature in precision elastic and inelastic electron scattering experiments and found to be extremely small [24], although the lack of non-linear contributions does not rule out a change to the slope that could explain the FFRP. The contribution of TPE to polarization transfer observables was also found to be small [25], as predicted by calculations [26, 27].

The TPE contribution to the cross section has the opposite sign for electron and positron scattering, making a comparison of positron-proton and electron-proton scattering one of the most direct tests for TPE. A global re-examination of  $e^+$ - $p$  and  $e^-$ - $p$  comparisons in 2003 showed evidence for TPE [28] at low  $Q^2$  values. After 2010, new experiments were performed to improve the precision and extend the kinematic range of these comparisons [29–31], finding evidence of a hard TPE effect in the ratio of  $e^+$ - $p$  and  $e^-$ - $p$  elastic scattering cross sections up to  $Q^2 \approx 2 \text{ (GeV/c)}^2$ .

While most proposed explanations of the FFRP focus on TPE, any  $\epsilon$ -dependent correction could contribute to that discrepancy, leading to updated examinations of the full radiative correction (RC) procedures, not just the TPE terms [32–34]. The most recent and complete update to the RC procedures [34] was applied to SLAC data from Refs. [4, 35]. The new RC procedures reduced the RS, but nonetheless provided a clear confirmation of the FFRP for  $Q^2$  from 4-7  $\text{(GeV/c)}^2$ . At higher  $Q^2$  the RS in elastic  $e$ - $p$  scattering has not previously been measured, because the previous data were collected only for forward angles, with insufficient range in  $\epsilon$  to constrain the RS.

Notwithstanding these experimental and theoretical efforts, the role of the TPE contribution is still not well understood (see reviews [36–38]). This work addresses the significance of the FFRP at much higher values of  $Q^2$  than previously investigated, and improves the precision of experimental constraints

on TPE effects in elastic  $e$ - $p$  scattering.

The experiment reported in the present work was conducted to obtain high-precision cross section measurements at large  $Q^2$  and relatively low values of  $\epsilon$ . These low- $\epsilon$  data, combined with existing high- $\epsilon$  measurements [5, 6, 35, 39], were used to extend Rosenbluth separations above 7  $\text{(GeV/c)}^2$ , and improve the precision of  $G_M$ . Finally, these measurements provide an important baseline for high- $Q^2$  measurements enabled by the 12 GeV upgrade at Jefferson Lab, where the measured cross sections are important for experimental normalization and cross checks, and for the broader program of high- $Q^2$  proton and neutron structure measurements.

This experiment, referred to hereafter as GMP12, was performed in Hall A of Jefferson Lab using the basic suite of experimental instrumentation [40]. A 100% duty-factor electron beam with current up to 68  $\mu\text{A}$  and energy from 2.2 to 11 GeV was incident on a 15-cm long liquid hydrogen target. The target operated at a temperature of 19 K, a pressure of 25 psia, and a density of 0.0732  $\text{g/cm}^3$ . The hydrogen target was complemented by a “dummy” cell consisting of two aluminum foils, used to measure the backgrounds originating from the entrance and exit windows of the hydrogen cell. The target density reduction with increasing beam intensity, due to localized boiling of the cryogen, was found to be 2.7% per 100  $\mu\text{A}$ , [41], with an estimated uncertainty of 0.35% in the variation of the correction across the current range of the experiment.

The energy of incident electrons was determined using the Hall A ARC energy measurement system, [42], which measures the field integral of the dipoles which bend the beam through 34.257 degrees from the accelerator into Hall A. These results were cross checked with spin precession studies and beam energy measurements in Hall C. The uncertainty in the beam energy was found to be less than 0.1% for all kinematics [43].

The beam current was measured by beam charge monitors (BCMs) [44], which were calibrated against a well-understood Unser monitor [45]. The uncertainty on the beam current and accumulated charge was defined by the accuracy of the BCM calibration. An absolute uncertainty of 0.06  $\mu\text{A}$  stems from the current source utilized to calibrate the Unser monitor. The latter results in an uncertainty of 0.1% at a current of 65  $\mu\text{A}$ , utilized for most of the GMP12 kinematics, and up to a maximum of 0.6% for the lowest current of 10  $\mu\text{A}$ .

The scattered electrons were detected in the left and right Hall A High Resolution Spectrometers (HRSSs), hereafter referred to as LHRS and RHRS, respectively. The HRSSs have a solid angle acceptance of 6.0 msr, momentum acceptance of  $\pm 4.5\%$ , intrinsic momentum resolution of  $2.5 \times 10^{-4}$ , and angular resolution of 0.6 mrad. The primary trigger was formed as a coincidence of signals in the front and back scintillator planes (separated by two meters) and the gas Cherenkov counter. The trigger efficiency was monitored using a sample of triggers that required only two of these three signals. For this experiment, the tracking system in each HRS was upgraded by adding a three-layer straw tube drift chamber to

allow accurate determination of the track reconstruction efficiency [46]. The particle identification detectors included a two-layer shower detector and a gas Cherenkov counter with enhanced light collection efficiency by means of a wavelength shifter [47]. Dead times of the trigger counters, front-end electronics, and DAQ were constantly measured using pulser generated events [41, 48].

The central momenta of the spectrometers were set to detect elastically scattered electrons. For calibration of the magnetic optics, data were collected from a target with 9 carbon foils separated by 3 cm along the beam line to define the scattering vertex position. To define the scattering angles, a 1 inch thick tungsten sieve slit with a 9 (vertical)  $\times$  7 (horizontal) hole pattern covering the angular acceptance was positioned in front of the first quadrupole magnet of each spectrometer [46, 48]. The direction of the electron beam and the spectrometer central angles were determined to 0.3 mrad precision by a series of geodesic surveys.

Several measurements were taken with the central spectrometer momentum above 3.1 GeV/c, where the magnetic flux in the first quadrupole magnet (Q1) begins to show saturation effects. Corrections to the nominal optics were determined for cases with saturated Q1, utilizing a model of the magnetic elements in COSY INFINITY [49] with a small additional uncertainty assigned to these cross sections of 0.5% in the worst case [44].

The cross section uncertainty due to the spectrometer acceptance was determined from detailed simulation studies in which the magnetic field integrals of each magnet, as well as the placement of each acceptance limiting aperture, were varied within their respective uncertainties. It was found [44] that the field and aperture uncertainties yield similar impact on the acceptance. Furthermore, high statistics runs in the LHRS at low  $Q^2$  were used for additional studies of the spectrometer acceptances, dead time of the data acquisition system, and event reconstruction efficiency [44, 46]. Based on these studies, we assign an acceptance uncertainty of 0.7% to each measurement and an overall cross section scale uncertainty of 0.8% for the LHRS data [44]. Because fewer studies were possible for the RHRS, an additional 1% scale uncertainty was assigned to these measurements.

Full simulations of the incident electron-target interaction and the electron trajectory through the HRS magnets and detectors were performed for each kinematic setting using an updated version of the magnetic optics Monte Carlo code [50] incorporating the HRSs. The event distributions in the detector package were compared with the simulated data and used to fine-tune the model of the HRS optical transport. All radiative processes were included in the Monte Carlo simulation using the procedure described in Ref. [51] based on an updated implementation [4] of the RC formalism of Ref. [52]. The uncorrelated systematic uncertainty of the GMp12 cross section data is 1.2-1.3%, while the overall scale uncertainty is 1.6% (2.0%) for the LHRS (RHRS) data.

The RC calculation of Refs. [32, 33] has the most accurate evaluation of the internal and external radiation, which is es-

sential for the analysis in the present work. The cross section measurements from GMp12 were adjusted accordingly (see Ref. [34] for details). The kinematics and reduced cross section results from the GMp12 experiment are shown in Table I.

TABLE I. Kinematics and reduced cross section values for the GMp12 measurements, with statistical and point-to-point systematic uncertainties added in quadrature. Points labeled with an asterisk (\*) were taken with the RHRS. There is an additional 1.6% (2.0%) scale uncertainty for the LHRS (RHRS) data, that is not included in the quoted uncertainties.

$E_e$ (GeV)	$\theta_e$ (deg)	$Q^2$ (GeV/c) <sup>2</sup>	$\epsilon$	$\sigma_R$
2.222	42.001	1.577	0.701	$(4.273 \pm 0.040) \times 10^{-2}$
2.222*	48.666	1.858	0.615	$(2.983 \pm 0.057) \times 10^{-2}$
6.427	24.250	4.543	0.826	$(3.813 \pm 0.057) \times 10^{-3}$
6.427	30.909	5.947	0.709	$(1.805 \pm 0.025) \times 10^{-3}$
6.427	37.008	6.993	0.599	$(1.113 \pm 0.016) \times 10^{-3}$
6.427	44.500	7.992	0.478	$(7.289 \pm 0.109) \times 10^{-4}$
8.518	30.909	9.002	0.648	$(5.163 \pm 0.078) \times 10^{-4}$
6.427*	55.900	9.053	0.332	$(4.859 \pm 0.107) \times 10^{-4}$
8.518	34.400	9.807	0.580	$(3.923 \pm 0.589) \times 10^{-4}$
8.518*	42.001	11.19	0.448	$(2.565 \pm 0.041) \times 10^{-4}$
8.518*	48.666	12.07	0.356	$(1.933 \pm 0.043) \times 10^{-4}$
8.518*	53.501	12.57	0.301	$(1.664 \pm 0.053) \times 10^{-4}$
10.587	48.666	15.76	0.309	$(8.405 \pm 0.227) \times 10^{-5}$

We combine our results with cross sections from several JLab and SLAC experiments [4–6, 20, 35, 39] spanning a  $Q^2$  range of 0.4-31 (GeV/c)<sup>2</sup> in a global fit of the  $Q^2$  and  $\epsilon$  dependence of the  $e$ - $p$  elastic scattering cross section using Eq. 2. Following Ref. [19], we exclude the forward angle data from Walker [4] and split the Andivahis [35] data set into two subsets, one for each spectrometer, and updated the cross section scale uncertainties of the data from the 1.6 GeV spectrometer. The experimental data included in the database, comprising 121 kinematic points, were chosen because the publications provide sufficient information on their RC procedures and cutoffs to allow us to self-consistently implement the RC modification [34]. The cross section database can be found in Ref. [53]. The normalizations of the data for the individual experiments were allowed to vary based on their quoted cross section scale uncertainties, except for the data of Ref. [20], which cover a wide range of  $Q^2$  with the best accuracy. The cross sections were fit in terms of  $G_M$  and RS with the following simple parametrizations, which provide sufficient flexibility at high  $Q^2$ :

$$\begin{aligned}
 G_M &= \mu_p (1 + a_1 \tau) / (1 + b_1 \tau + b_2 \tau^2 + b_3 \tau^3), \\
 RS &= 1 + c_1 \tau + c_2 \tau^2.
 \end{aligned}
 \tag{3}$$

The optimal values of the parameters and uncertainties are given in Tab. II.

Figure 1 shows the global fit to  $G_M$  along with the  $G_M$  values extracted from the individual cross section measurements, using the global fit to RS( $Q^2$ ) to extrapolate to  $\epsilon = 0$  and isolate  $G_M$ . In the global fit, the inclusion of our new data de-

TABLE II. Global fit results for the parameters describing the proton magnetic form factor  $G_M$  and the Rosenbluth slope RS.

$a_1$	$b_1$	$b_2$	$b_3$	$c_1$	$c_2$
0.072(22)	10.73(11)	19.81(17)	4.75(65)	-0.46(12)	0.12(10)

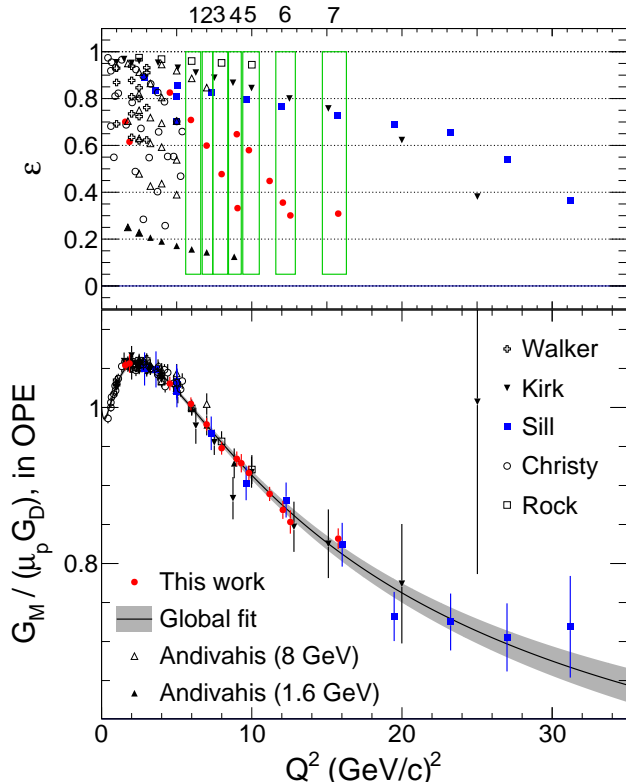


FIG. 1. (Top) Kinematics of elastic  $e$ - $p$  cross section data used in the global fit and Rosenbluth separations; the boxes (1-7) indicate the groupings of points for the Rosenbluth separations. (Bottom) The effective proton magnetic form factor, normalized by the standard dipole  $\mu_p G_D$ , obtained from the cross section measurements of GMp12 and Refs. [4–6, 20, 35, 39], with symbols as indicated in the plot’s legend. The curve shows the result of our global fit, with the gray shaded area indicating the 68% confidence interval.

creases the uncertainties in the extraction of  $G_M$  by 30% or more for  $Q^2 > 6$  (GeV/c) $^2$ .

A model-independent determination of the Rosenbluth slope requires at least two measurements at identical  $Q^2$  values. In practice, even closely located measurements have some differences in  $Q^2$ , requiring interpolation. In our analysis, data with similar  $Q^2$  values were grouped as indicated by the boxes in the top panel of Fig. 1. The normalization resulting from the global fit was applied to each data set, modifying the cross sections from Table I. The individual data points were then interpolated to a central  $Q^2$  value,  $Q_c^2$ ; the detailed extraction procedure including treatment of the relative normalization between different experiments is described in Ref. [53]. The interpolated data points were then used in lin-

ear fits to the  $\varepsilon$  dependence of  $\sigma_R(Q_c^2, \varepsilon)$  to determine  $G_M$  and RS at seven  $Q^2$  values, as given in Table III. Figure 2 shows  $\sqrt{RS}$  (yielding  $\mu_p G_E/G_M$  in the OPE) from our global analysis, along with a fit to the polarization data. The L/T results are consistent with approximate form factor scaling.

TABLE III. Rosenbluth separation results for the data groupings shown in the top panel of Fig. 1, after centering to the average  $Q_c^2$ . The quoted values of  $\sigma_L$  and  $\sigma_T$  as defined in Eq. 2, and  $G_M/(\mu_p G_D)$  and  $\mu_p G_E/G_M$  are obtained assuming validity of the one-photon-exchange approximation. For the largest  $Q^2$  value, where  $\sigma_L$  is negative, we quote  $-\sqrt{|RS|}$ .

$Q_c^2$ (GeV/c) $^2$	$\sigma_T \times 10^5$	$\sigma_L \times 10^5$	$G_M/(\mu_p G_D)$ (OPE)	$\mu_p G_E/G_M$ (OPE)
5.994	$167 \pm 4$	$7.1 \pm 4.6$	$1.000 \pm 0.011$	$0.75 \pm 0.25$
7.020	$104 \pm 3$	$9.3 \pm 5.3$	$0.967 \pm 0.015$	$1.18 \pm 0.35$
7.943	$71.0 \pm 2.7$	$4.1 \pm 3.9$	$0.943 \pm 0.018$	$1.0 \pm 0.5$
8.994	$49.8 \pm 1.7$	$0.7 \pm 3.0$	$0.934 \pm 0.016$	$0.5 \pm 1.2$
9.840	$36.9 \pm 2.4$	$1.9 \pm 3.5$	$0.909 \pm 0.029$	$1.1 \pm 1.0$
12.249	$18.0 \pm 0.8$	$1.2 \pm 1.8$	$0.858 \pm 0.019$	$1.3 \pm 1.1$
15.721	$8.6 \pm 0.5$	$-0.2 \pm 1.2$	$0.840 \pm 0.025$	$(-0.9 \pm 2.8)$

While it is conventional to compare Rosenbluth and polarization data by showing  $\mu_p G_E/G_M$ , it is more correct to compare the results in terms of the quantities most directly measured in the experiment. Thus, to extract the impact of TPE we make a direct comparison of the extracted RS to the value expected from the polarization fit to  $\mu_p G_E/G_M$ , as detailed in the supplemental material [53].

Based on our global fit, we find that the TPE null hypothesis has a discrepancy with the experimental data above  $2\sigma$  up to 8 GeV $^2$  and above  $1\sigma$  up to 14 GeV $^2$ , compared to 6 GeV $^2$  and 8 GeV $^2$  without our new data. Because this is a fit-dependent statement, we also examine the direct L/T separations which are essentially independent of the global fit. We take the measured RS value minus the value predicted by the fit to PT data, and find that the excess in RS associated with TPE is  $2\sigma$  from zero when taken as a constant shift in RS as a function in  $Q^2$ . We also obtain a  $2\sigma$  deviation from the polarization result if we assume that the change in RS is proportional to  $\tau$ , as expected if the observed slope is dominated by TPE rather than the  $G_E$  contribution and the TPE contributions are nearly constant at large  $Q^2$ .

In summary, the  $e$ - $p$  elastic scattering cross section was measured for beam energies in the range of 2.2 - 11 GeV and  $Q^2$  up to 15.75 (GeV/c) $^2$ . Data from this experiment were combined with other cross section measurements [4–6, 35, 39] to perform Rosenbluth separations in a new  $Q^2$  regime. The observed difference between the measured Rosenbluth slope and the OPE expectation, with  $G_E/G_M$  from polarization transfer, unambiguously shows significant TPE contributions to the  $e$ - $p$  elastic scattering cross section. These new, precise cross section data provide an important baseline for the future proton and neutron structure investigations in the Jefferson Lab 12 GeV program.

We thank the Jefferson Lab accelerator and Hall A technical

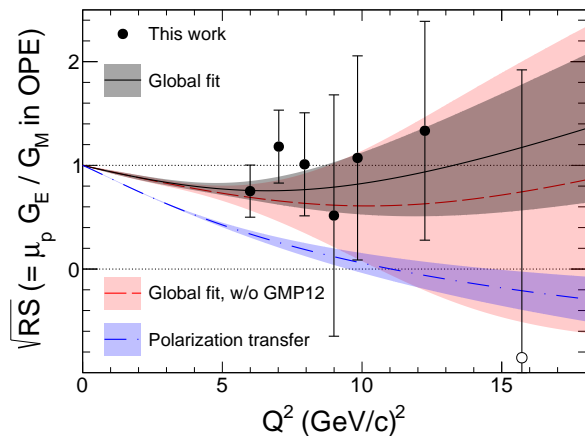


FIG. 2. Direct Rosenbluth separation results for  $\sqrt{RS}$  ( $= \mu_p G_E / G_M$  in OPE). The black solid (red dashed) curve shows the results of our fit to the cross section data with (without) the new GMP12 data. The blue dot-dashed curve shows  $\mu_p G_E / G_M$  from a fit to the polarization data [53]. The shaded bands show the 68% confidence intervals of the respective fits. Following the convention of Tab. III, we plot  $-\sqrt{|RS|}$  for the highest  $Q^2$  point (an open circle), where  $RS < 0$ .

staff for their outstanding support of this experiment, which was part of the first run group to take data at JLab after the accelerator upgrade. We thank N. Kivel for careful reading of the manuscript and his valuable suggestions. Communications with P.N. Kirk, S. Rock, and A. Sill about technical aspects of their experiments are very much appreciated. This work was supported in part by the UK Science and Technology Facilities Council (Grant nos. STFC 57071/1 and STFC 50727/1), the U.S. National Science Foundation grant PHY-1508272, and the U.S. Department of Energy, Office of Science, Office of Nuclear Physics under contracts DE-AC02-05CH11231, DE-AC02-06CH11357, and DE-SC0016577, the Natural Sciences and Engineering Research Council of Canada (NSERC), and DOE contract DE-AC05-06OR23177, under which JSA, LLC operates JLab.

\* Contact person, bogdanw@jlab.org

[1] M. N. Rosenbluth, *Physical Review* **79**, 615 (1950).

[2] R. Sachs, *Phys. Rev.* **126**, 2256 (1962).

[3] R. Hofstadter, *Rev. Mod. Phys.* **28**, 214 (1956).

[4] R. C. Walker *et al.*, *Phys. Rev.* **D49**, 5671 (1994).

[5] P. N. Kirk *et al.*, *Phys. Rev.* **D8**, 63 (1973).

[6] A. F. Sill *et al.*, *Phys. Rev.* **D48**, 29 (1993).

[7] G. P. Lepage and S. J. Brodsky, *Phys. Rev. Lett.* **43**, 545 (1979), [Erratum: *Phys. Rev. Lett.* **43**, 1625 (1979)]; *Phys. Rev.* **D22**, 2157 (1980).

[8] A. I. Akhiezer, L. N. Rozentsveig, and I. M. Shumushkevich, *Soviet Physics JETP* **6**, 588 (1958), *Zhurnal Eksperimental'noi i Teoreticheskoi Fiziki*, **33**, 765 (1957); A. I. Akhiezer and M. Rekalov, *Sov. Phys. Dokl.* **13**, 572 (1968), [*Dokl. Akad. Nauk Ser. Fiz.* **180**, 1081 (1968)]; *Sov. J. Part. Nucl.* **4**, 277 (1974), [*Fiz. Elem. Chast. Atom. Yadra* **4**, 662 (1973)].

[9] G. Frolov, *Soviet Physics JETP* **7**, 525 (1958).

[10] J. H. Scofield, *Phys. Rev.* **113**, 1599 (1959); *Phys. Rev.* **141**, 1352 (1966).

[11] R. G. Arnold, C. E. Carlson, and F. Gross, *Phys. Rev.* **C23**, 363 (1981).

[12] M. K. Jones *et al.* (Jefferson Lab Hall A), *Phys. Rev. Lett.* **84**, 1398 (2000), arXiv:nucl-ex/9910005 [nucl-ex]; O. Gayou *et al.* (Jefferson Lab Hall A), *Phys. Rev. Lett.* **88**, 092301 (2002), arXiv:nucl-ex/0111010; V. Punjabi *et al.*, *Phys. Rev.* **C71**, 055202 (2005), [Erratum: *Phys. Rev.* **C71**, 069902 (2005)], arXiv:nucl-ex/0501018 [nucl-ex].

[13] A. J. R. Puckett *et al.*, *Phys. Rev.* **C85**, 045203 (2012), arXiv:1102.5737 [nucl-ex].

[14] A. J. R. Puckett *et al.*, *Phys. Rev. Lett.* **104**, 242301 (2010), arXiv:1005.3419 [nucl-ex]; *Phys. Rev.* **C96**, 055203 (2017), [erratum: *Phys. Rev.* **C98**, no.1, 019907 (2018)], arXiv:1707.08587 [nucl-ex].

[15] G. A. Miller and M. R. Frank, *Phys. Rev.* **C65**, 065205 (2002), arXiv:nucl-th/0201021 [nucl-th]; A. V. Belitsky, X.-d. Ji, and F. Yuan, *Phys. Rev. Lett.* **91**, 092003 (2003), arXiv:hep-ph/0212351 [hep-ph].

[16] C. D. Roberts, M. S. Bhagwat, A. Holl, and S. V. Wright, *Eur. Phys. J. ST* **140**, 53 (2007), arXiv:0802.0217 [nucl-th]; I. C. Cloet, G. Eichmann, B. El-Bennich, T. Klahn, and C. D. Roberts, *Few Body Syst.* **46**, 1 (2009), arXiv:0812.0416 [nucl-th]; M. Y. Barabanov *et al.*, *Prog. Part. Nucl. Phys.* **116**, 103835 (2021), arXiv:2008.07630 [hep-ph].

[17] B. Wojtsekhowski, W. Bertozzi, K. Fissum, and D. Rowntree, report Jefferson Lab PAC15, Appendix E, LOI-99-003 (1999).

[18] R. Segel and J. Arrington, report Jefferson Lab PAC19, Individual Proposal Report, E-01-001 (2001).

[19] J. Arrington, *Phys. Rev.* **C68**, 034325 (2003), arXiv:nucl-ex/0305009 [nucl-ex]; *Phys. Rev. C* **69**, 022201 (2004), arXiv:nucl-ex/0309011.

[20] M. E. Christy *et al.* (E94110), *Phys. Rev.* **C70**, 015206 (2004), arXiv:nucl-ex/0401030 [nucl-ex].

[21] I. A. Qattan *et al.*, *Phys. Rev. Lett.* **94**, 142301 (2005), arXiv:nucl-ex/0410010 [nucl-ex].

[22] P. G. Blunden, W. Melnitchouk, and J. A. Tjon, *Phys. Rev. Lett.* **91**, 142304 (2003), arXiv:nucl-th/0306076 [nucl-th].

[23] P. A. M. Guichon and M. Vanderhaeghen, *Phys. Rev. Lett.* **91**, 142303 (2003), arXiv:hep-ph/0306007 [hep-ph].

[24] V. Tsvaskis, J. Arrington, M. E. Christy, R. Ent, C. E. Keppel, Y. Liang, and G. Vittorini, *Phys. Rev.* **C73**, 025206 (2006), arXiv:nucl-ex/0511021 [nucl-ex].

[25] M. Meziane *et al.*, *Phys. Rev. Lett.* **106**, 132501 (2011).

[26] D. Borisyuk and A. Kobushkin, *Phys. Rev.* **C90**, 025209 (2014), arXiv:1405.2467 [hep-ph].

[27] P. G. Blunden, W. Melnitchouk, and J. A. Tjon, *Phys. Rev.* **C72**, 034612 (2005), arXiv:nucl-th/0506039 [nucl-th].

[28] J. Arrington, *Phys. Rev.* **C69**, 032201 (2004), arXiv:nucl-ex/0311019 [nucl-ex].

[29] I. A. Rachek *et al.*, *Phys. Rev. Lett.* **114**, 062005 (2015), arXiv:1411.7372 [nucl-ex].

[30] D. Adikaram *et al.* (CLAS), *Phys. Rev. Lett.* **114**, 062003 (2015), arXiv:1411.6908 [nucl-ex]; D. Rimal *et al.* (CLAS), *Phys. Rev.* **C95**, 065201 (2017), arXiv:1603.00315 [nucl-ex].

[31] B. S. Henderson *et al.* (OLYMPUS), *Phys. Rev. Lett.* **118**, 092501 (2017), arXiv:1611.04685 [nucl-ex].

[32] L. C. Maximon and J. A. Tjon, *Phys. Rev.* **C62**, 054320 (2000), arXiv:nucl-th/0002058 [nucl-th].

[33] R. Gerasimov and V. Fadin, *Phys. Atom. Nucl.* **78**, 69 (2015).

[34] A. V. Gramolin and D. M. Nikolenko, *Phys. Rev.* **C93**, 055201 (2016), arXiv:1603.06920 [nucl-ex].

- [35] L. Andivahis *et al.*, *Phys. Rev.* **D50**, 5491 (1994).
- [36] J. Arrington, P. G. Blunden, and W. Melnitchouk, *Prog. Part. Nucl. Phys.* **66**, 782 (2011), arXiv:1105.0951 [nucl-th].
- [37] A. Afanasev, P. Blunden, D. Hasell, and B. Raue, *Prog. Part. Nucl. Phys.* **95**, 245 (2017), arXiv:1703.03874 [nucl-ex].
- [38] Z. Ye, J. Arrington, R. J. Hill, and G. Lee, *Phys. Lett. B* **777**, 8 (2018), arXiv:1707.09063 [nucl-ex].
- [39] S. Rock *et al.*, *Phys. Rev. D* **46**, 24 (1992).
- [40] J. Alcorn *et al.*, *Nucl. Instrum. Meth.* **A522**, 294 (2004).
- [41] B. Schmookler, *Nucleon Structure and Its Modification in Nuclei*, *Ph.D. thesis*, Massachusetts Institute of Technology (2018).
- [42] J. Berthot and P. Vernin, *Nucl. Phys. News* **9N4**, 12 (1999).
- [43] S. Santiesteban, L. Tracy, and D. Higinbotham, “Precision beam energy determination for the cebaF 12 GeV upgrade,” (2020), in preparation for publication in *Nucl. Instrum. and Meth. A*.
- [44] T. Gautam, *Precision Measurement of the Proton Magnetic Form Factor at high  $Q^2$* , *Ph.D. thesis*, Hampton University, Hampton, Virginia (2019).
- [45] K. Unser, *Application of accelerators in Research and Industry, Proceedings, 6th conference, Denton, Texas, USA, November 3-5, 1980*, *IEEE Trans. Nucl. Sci.* **28**, 2344 (1981).
- [46] Y. Wang, *Measurement of the Proton Elastic Cross Section at  $Q^2 = 0.66, 1.10, 1.51$  and  $1.65$  GeV<sup>2</sup>*, *Ph.D. thesis*, College of William & Mary (2017).
- [47] K. Allada, C. Hurlbut, L. Ou, B. Schmookler, A. Shahinyan, and B. Wojtsekhowski, *Nucl. Instrum. Meth.* **A782**, 87 (2015), arXiv:1502.01772 [physics.ins-det].
- [48] L. Ou, *Precision Measurements of Electron-Proton Elastic Scattering Cross Sections at Large  $Q^2$* , *Ph.D. thesis*, Massachusetts Institute of Technology (2018).
- [49] K. Makino and M. Berz, *Computational accelerator physics. Proceedings, 8th International Conference, ICAP 2004, St. Petersburg, Russia, June 29-July 2, 2004*, *Nucl. Instrum. Meth.* **A558**, 346 (2006).
- [50] J. Arrington, *Inclusive Electron Scattering From Nuclei at  $x > 1$  and High  $Q^2$* , *Ph.D. thesis*, California Institute of Technology (1998), arXiv:nucl-ex/0608013.
- [51] R. Ent, B. W. Filippone, N. C. R. Makins, R. G. Milner, T. G. O’Neill, and D. A. Wasson, *Phys. Rev. C* **64**, 054610 (2001).
- [52] L. W. Mo and Y.-S. Tsai, *Rev. Mod. Phys.* **41**, 205 (1969).
- [53] “See supplemental material at [url will be inserted by publisher] for the data base and the global fit of the e-p cross section data.”